Asymmetric Inter-Eye Progression in Stargardt Disease

Stanley Lambertus,[1] Nathalie M. Bax,[1] Joannes M. M. Groenewoud,[2] Frans P. M. Cremers,[3] Gert Jan van der Wilt,[2] B. Jeroen Klevering,[1] Thomas Theelen,[1] and Carel B. Hoyng[1]

[1]Department of Ophthalmology, Donders Institute for Brain, Cognition and Behaviour, Radboud University Medical Center, Nijmegen, The Netherlands
[2]Department for Health Evidence, Donders Institute for Brain, Cognition and Behaviour, Radboud University Medical Center, Nijmegen, The Netherlands
[3]Department of Human Genetics, Donders Institute for Brain, Cognition and Behaviour, Radboud University Medical Center, Nijmegen, The Netherlands

Correspondence: Carel B. Hoyng, Department of Ophthalmology (400), Radboud University Medical Center, P.O. Box 9101, 6500 HB Nijmegen, The Netherlands; carel.hoyng@radboudumc.nl.

Submitted: October 21, 2016
Accepted: November 16, 2016

Citation: Lambertus S, Bax NM, Groenewoud JMM, et al. Asymmetric inter-eye progression in Stargardt disease. *Invest Ophthalmol Vis Sci*. 2016;57:6824–6830. DOI:10.1167/iovs.16-20963

Purpose. Asymmetry in disease progression between left and right eyes can occur in Stargardt disease (STGD1), and this needs to be considered in novel therapeutic trials with a fellow-eye paired controlled design. This study investigated the inter-eye discordance of best-corrected visual acuity (BCVA) and progression of RPE atrophy in STGD1.

Methods. We performed a retrospective cohort study collecting 68 STGD1 patients (136 eyes) with $\geq$1 *ABCA4* variants and $\geq$0.5-year follow-up on BCVA and fundus autofluorescence. We compared inter-eye correlations of RPE atrophy progression between early-onset ($\leq$10 years), intermediate-onset (11–44), and late-onset ($\geq$45) STGD1 and *ABCA4* variant combinations by χ^2 tests. We identified associations of discordant baseline BCVA and RPE atrophy with discordant RPE atrophy progression by odds ratios (OR). We defined discordance by differences >1.5 interquartile ranges ± first/third interquartiles.

Results. Progression of RPE atrophy correlated moderately between eyes ($\rho = 0.766$), which decreased with later onset ($P = 9.8 \times 10^{-7}$) and lower pathogenicity of *ABCA4* combinations ($P = 0.007$). Twelve patients (17.6%) had discordant inter-eye RPE atrophy progression, associated with baseline discordance of RPE atrophy (OR, 6.50 [1.35–31.34]), but not BCVA (OR, 0.33 [0.04–2.85]).

Conclusions. Lower inter-eye correlations are more likely found in late-onset STGD1 and patients carrying low pathogenic *ABCA4* combinations. To achieve the highest power in a therapeutic trial, early-phase studies should minimize inter-eye discordance by selecting early-onset STGD1 patients carrying severe *ABCA4* variants without evidence of asymmetry at baseline.

Keywords: inter-eye correlation, asymmetry, RPE atrophy, Stargardt

Stargardt disease (STGD1) is one of the most common retinal dystrophies. Loss of macular function causes bilateral loss of visual acuity, usually at childhood.[1,2] The first manifestations of the disease may also occur in older patients, up to the seventh decade.[3,4] In general, the severity of the disease is associated with the age of onset; young patients tend to do worse.[5] The variation in age of onset and rate of progression is, for the most part, the result of combinations of over 900 variants in the *ABCA4* gene.[6]

ABCA4 encodes the adenosine triphosphate-binding cassette, subfamily A, member 4 transporter protein, which actively removes all-*trans*-retinal with its conjugate *N*-retinylidene-phosphatidylethanolamine from the photoreceptor outer segment disks.[7] Impaired removal results in condensation reactions, which lead to toxic levels of bisretinoids in the outer segment disks. Through phagocytosis of these outer segments, bisretinoids accumulate as lipofuscin deposits in the RPE. These lipofuscin deposits are observed as yellowish-white flecks in the posterior pole.[8] The accumulation of toxic lipofuscin eventually leads to atrophy of the RPE and photoreceptors with subsequent loss of the neurosensory retina and choriocapillaris.[9]

Over time, RPE atrophy progresses, as uni- or multifocal areas enlarge and coalesce. However, there is considerable variability in these patterns of atrophy; they range from large central atrophic areas in early-onset STGD1 patients that can be seen at adolescence[2] to relatively small atrophic lesions encircling the fovea in older patients with late-onset STGD1.[3] The difference in atrophic lesion not only varies between patients,[10] but also the patterns of RPE loss may differ significantly between eyes of one patient. Even though the extent of abnormalities is often similar between left and right eyes,[11,12] some cases with remarkable differences have been described.[13]

Profound inter-eye differences in disease progression have impact on the statistical power in clinical trials; treated and untreated eyes must demonstrate a larger difference than do the inter-eye differences by their natural course. Otherwise, the required sample size will be unreasonably large. However, in early-phase clinical trials for novel treatments of STGD1[14–16] and other retinal dystrophies, small therapeutic effects have to be evaluated, generally within 2 years, with no more than a few dozen patients. Thus, better knowledge of inter-eye correlations is needed for fellow-eye paired controlled trials in which the untreated eyes of participants serve as a control.

In view of these upcoming interventional trials, we have studied the extent of asymmetric inter-eye progression of RPE

This work is licensed under a Creative Commons Attribution-NonCommercial-NoDerivatives 4.0 International License.
Downloaded from iovs.arvojournals.org on 06/28/2019

atrophy in patients with STGD1. Fundus autofluorescence (FAF) imaging is a valuable tool to evaluate progression of RPE atrophy over time.[17–20] We therefore analyzed inter-eye discordance of RPE atrophy progression using FAF imaging along with visual acuity. We hypothesized that a later disease onset and less pathogenic combinations of *ABCA4* variants contribute to asymmetric inter-eye progression and that the asymmetry will increase when asymmetry at baseline is already present.

Methods

Patient Selection

We selected patients from the STGD1 database, containing 454 cases, of the Department of Ophthalmology at Radboud University Medical Center (Nijmegen, The Netherlands). We included patients in whom the clinical diagnosis of STGD1 was supported by the presence of ≥1 (likely) pathogenic *ABCA4* variants with a follow-up data of ≥6 months on FAF imaging. Ninety-three STGD1 patients met these inclusion criteria.

Ten cases were excluded because no RPE atrophy had developed during the entire follow-up time. Nine cases displayed RPE atrophy to such a degree that the lesions extended beyond the limits of the FAF image. One case was excluded because choroidal neovascularization occurred in one eye. Five cases were excluded because they participated in an interventional trial.[21] The remaining 68 cases were included in this study. The patient inclusion process is shown in Supplementary Figure S1. This retrospective cohort study was approved by the Institutional Ethics Committee and was performed in accordance with the Declaration of Helsinki.

Measurements

We documented sex, age at onset, age at baseline, and follow-up time. Age at onset was defined as either the age at which visual complaints were first noted, or if unavailable, the age when the diagnosis was made. Disease-onset groups were based on previously reported cut-off points: early-onset STGD1, ≤10 years,[2] and late-onset STGD1, ≥45 years.[3] The remaining patients were grouped as intermediate-onset STGD1, 11 to 44 years. The age at baseline was the first visit with available imaging and visual acuity tests.

Best-corrected visual acuity (BCVA) was measured with a Snellen or Early Treatment Diabetic Retinopathy Study chart, then transformed into the logarithm of the minimum angle of resolution (logMAR) for analysis. Fundus autofluorescence ($\lambda =$ 488 nm, emission 500–700 nm) imaging was performed using a confocal scanning laser ophthalmoscope (Spectralis HRA-OCT; Heidelberg Engineering, Heidelberg, Germany). The field of view was set at $30^\circ \times 30^\circ$ or $55^\circ \times 55^\circ$ and was centered on the macula.[22]

Image Quantification

The total RPE atrophy area was automatically quantified in FAF images by an observer-independent image analysis algorithm. The algorithm automatically segmented the area starting from an arbitrarily selected seed point inside the atrophic area. This method was based on a combination of a region-growing algorithm and a dynamic, user-independent threshold selection procedure using Otsu thresholding. Areas were square root ($\surd$) transformed to correct for baseline RPE atrophy area.[23] A good agreement has previously been observed between manual area measurements and the automatically quantified values (Sanchez CI, et al. *IOVS* 2015;56:ARVO E-Abstract 5258) and was found to be consistent with the agreement within this cohort (intra-class correlation coefficient, 0.977; 95% confidence interval [CI], 0.951–0.987).

Genetic Analysis

All reported *ABCA4* variants (Supplementary Table S1) were classified as follows: (1) pathogenic: truncating alleles, significantly enriched in *ABCA4*-LOVD (http://www.LOVD.nl/ABCA4, in the public domain), which contains 6903 variants (861 unique variants) reported in 3987 persons with STGD1 or autosomal recessive cone-rod dystrophy (Cornelis SS, Cremers FPM, unpublished data, 2016); (2) likely pathogenic: non-truncating alleles, significantly enriched in *ABCA4*-LOVD; (3) likely benign: allele frequency (AF) *ABCA4*-LOVD/AF ExAC non-Finnish Caucasian <1; (4) benign: ExAC AF >0.006; (5) unknown pathogenicity: AF *ABCA4*-LOVD/AF ExAC non-Finnish Caucasian >1, however not significantly enriched. Patients were then grouped by combinations of *ABCA4* pathogenicity: (1) pathogenic/pathogenic; (2) pathogenic/likely pathogenic; (3) likely pathogenic/likely pathogenic; (4) pathogenic in combination with unknown pathogenicity, (likely) benign, or a variant that was not published until December 31, 2015; (5) likely pathogenic in combination with unknown pathogenicity or (likely) benign (Cornelis SS, Cremers FPM, unpublished data, 2016).

Statistical Analysis

We analyzed BCVA and RPE atrophy measurements using analysis software (SPSS version 22; IBM Corp., IBM SPSS Statistics, Chicago, IL, USA) with parametric tests. Retinal pigment epithelium atrophy progression rates were calculated by the difference at the baseline and last follow-up visit divided by the follow-up time. Differences in disease duration and follow-up time between disease-onset groups were analyzed with the Kruskal-Wallis test.

We used Pearson's correlation coefficients (ρ) to assess inter-eye correlations of baseline BCVA, baseline RPE atrophy, and RPE atrophy progression. We compared these correlations between disease-onset groups and *ABCA4* variant combination groups by first performing a Fisher transformation:

$$z' = \frac{1}{2}\ln\frac{1+\rho}{1-\rho}. \quad (1)$$

Then, these z' scores were compared for homogeneity. The test for homogeneity employs the χ^2 distribution for two and four degrees of freedom:

$$\chi^2 = \sum (n_i - 3)(z_i'^2) - \frac{\left[\sum (n_i - 3)(z_i')\right]^2}{\sum (n_i - 3)} \quad (2)$$

where the summation is over the three disease-onset groups and five *ABCA4* variant combination groups, respectively.[24]

Baseline BCVA and RPE atrophy differences between measurements and the average measurements of both eyes were calculated and plotted according to the method of Bland and Altman to assess the intra-individual agreement graphically.[25] Limits of agreement between eyes were plotted for each disease-onset group.

Lin's concordance correlation coefficient ρ_c was calculated to evaluate the extent of inter-eye symmetry of baseline BCVA, baseline RPE atrophy, and RPE atrophy progression.[26–28] The ρ_c consists of the product of a precision coefficient (Pearson's ρ) and an accuracy coefficient χ_α. The accuracy coefficient χ_α indicates how far the best-fit line of all paired left- and right-eye measurements deviates from the 45° line on a square scatter

Investigative Ophthalmology & Visual Science

Downloaded from iovs.arvojournals.org on 06/28/2019

Table 1. Characteristics and Inter-Eye correlations at Baseline and at Follow-up in 68 Stargardt Patients

Patient Characteristics	Early-Onset STGD1	Intermediate-Onset STGD1	Late-Onset STGD1	*P* Value
Sex	7 male 7 female	9 male 24 female	10 male 11 female	
Age at onset, y (median and range)	8.5 (4–10)	20 (11–42)	50 (45–69)	
Baseline				
Disease duration, y (median and range)	7 (0–27)	4 (0–39)	5 (0–26)	0.768*
Age, y (median and range)	14.5 (9–31)	36 (13–56)	59 (45–81)	
BCVA, logMAR (mean and SD)				0.419†
OD	1.08 (±0.41)	0.67 (0.50)	0.36 (±0.39)	
OS	1.09 (±0.28)	0.77 (0.49)	0.40 (±0.55)	
Correlation, ρ	0.830	0.723	0.619	
$\surd$ RPE atrophy, mm (mean and SD)				5.5×10^{-8}†
OD	1.79 (±1.29)	1.31 (±1.52)	1.79 (±1.10)	
OS	1.76 (±1.27)	1.28 (±1.58)	1.51 (±1.03)	
Correlation, ρ	0.992	0.931	0.601	
Follow-up				
Follow-up time, y (median and range)	5.7 (1.1–9.7)	3.1 (0.9–9.5)	3.8 (0.5–7.6)	0.220*
Age, y (median and range)	21 (11–36)	33 (15–59)	64 (47–86)	
BCVA, logMAR (mean and SD)				0.0497†
OD	1.23 (±0.29)	0.93 (±0.44)	0.63 (±0.60)	
OS	1.23 (±0.29)	0.88 (±0.52)	0.54 (±0.60)	
Correlation, ρ	0.897	0.767	0.527	
$\surd$ RPE atrophy, mm (mean and SD)				6.1×10^{-4}†
OD	2.73 (±1.23)	1.89 (±1.69)	2.29 (±1.55)	
OS	2.77 (±1.26)	1.86 (±1.62)	2.17 (±1.49)	
Correlation, ρ	0.974	0.938	0.670	

Median and ranges are shown for time variables. Mean and standard deviations (SD) are shown for BCVA and $\surd$ RPE atrophy.
* Kruskal-Wallis test for differences in disease duration and follow-up.
† χ^2 With two degrees of freedom for differences in inter-eye correlations.

plot and is defined as $\frac{2}{\varpi+1/\varpi+v^2}$, where scale shift $\varpi = \sigma_{OD}/\sigma_{OS}$ and location shift relative to the scale is $v = \frac{\mu_{OD}-\mu_{OS}}{\sqrt{\sigma_{OD}\sigma_{OS}}}$ (OD, right eye; OS, left eye).[29] If all paired measurements exactly lie on the 45° line, a coefficient of 1 would be found, indicating perfect symmetry. Strength-of-agreement criteria were as follows: almost perfect, >0.90; substantial, 0.80–0.90; moderate, 0.65–0.80; poor, <0.65.[30]

As standard deviations can be affected by extreme differences and rely on distributional assumptions, box and whisker plots were used to identify outliers by differences >1.5 interquartile ranges (IQR) below the first (Q_1) or above the third (Q_3) interquartiles in baseline BCVA, baseline RPE atrophy, and RPE atrophy progression. Odds ratios were calculated to identify associations of discordant BCVA and RPE atrophy at baseline with RPE atrophy progression.

We performed sample-size calculations and a sensitivity analysis for a theoretical intervention using nQuery Advisor 7.0 (Statistical Solutions, Boston, MA, USA). We used a two-sided paired *t*-test for differences in means of RPE atrophy progression with a test significance level (α) of 0.05 and a power of ($1 - \beta$) of 0.80. Standard deviations of differences between RPE atrophy progression of treated and nontreated eyes were obtained from the standard deviations and correlations of left and right eyes using the formula $\sigma_d = \sqrt{(\sigma_1{}^2 + \sigma_2{}^2 - 2\rho\sigma_1\sigma_2)}$.

Results

Patient Characteristics

A total of 68 patients (136 eyes) were included in this study (26 men and 42 women). The median age at onset was 8.5 (range, 4–10), 20 (range, 11–42), and 50 (range, 45–69) years for 14 early-onset STGD1, 33 intermediate-onset STGD1, and 21 late-onset STGD1 patients, respectively. At baseline, the median disease duration was 5 years (range, 0–39). The distribution did not differ between the three disease-onset categories. Details of patient characteristics and inter-eye correlations at baseline and follow-up are depicted in Table 1.

Baseline Inter-Eye Correlations of Best-Corrected Visual Acuity. At baseline, the mean (± standard deviation) BCVA in the right and left eyes was 0.66 (±0.51) logMAR and 0.72 (±0.53) logMAR, respectively. Twenty-four right eyes and 23 left eyes were identified as the better-seeing eye; 21 pairs of eyes had equal BCVA. The overall inter-eye correlation (ρ) in BCVA at baseline was 0.756 and did not differ between disease-onset groups, although a trend of decreasing correlations at later disease-onset was also observed at follow-up.

Next, we compared the average and differences of baseline BCVA between the left and right eyes by a Bland-Altman plot (Supplementary Fig. S2A), revealing discordance up to 1.70 logMAR. This discordance was most pronounced in 13 patients (two early-onset STGD1, seven intermediate-onset STGD1, and four late-onset STGD1), as defined by outlying differences below $Q_1 - 1.5 \times IQR$ or above $Q_3 + 1.5 \times IQR$ (Supplementary Fig. S2B). Overall, this resulted in an inter-eye agreement (ρ_c) in baseline BCVA of 0.751 (95% confidence interval (CI), 0.626–0.838).

Baseline Inter-Eye Correlations of RPE Atrophy. At baseline, the mean $\surd$ RPE atrophy area in the right and left eyes was 1.56 mm (±1.36) and 1.45 mm (±1.36), respectively. Twenty-nine right eyes and 34 left eyes had the smallest RPE atrophy area; 5 pairs of eyes had no RPE atrophy. Although baseline RPE atrophy between the left and right eyes was highly correlated ($\rho = 0.878$), the correlation was significantly decreased in late-onset STGD1 patients.

Investigative Ophthalmology & Visual Science

Downloaded from iovs.arvojournals.org on 06/28/2019

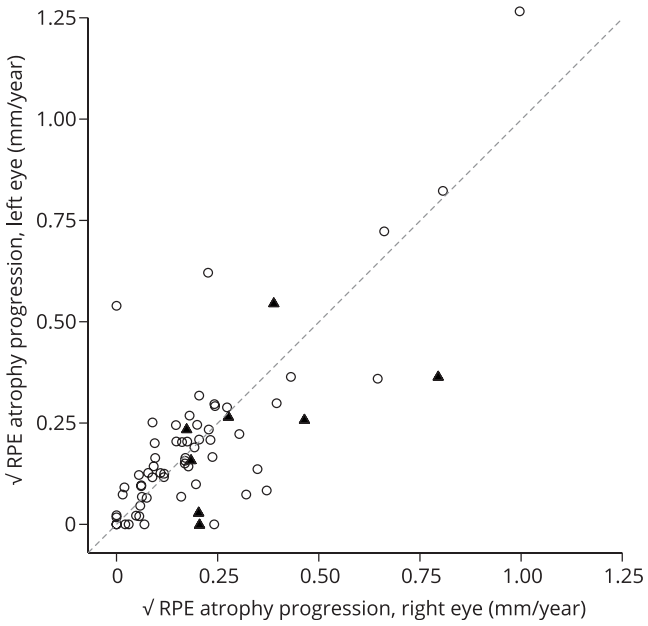

Figure 1. A square scatter plot of inter-eye √ RPE progression. *Circles* are patients with differences in baseline √ RPE atrophy between their eyes within $Q_{1,3} \pm 1.5 \times IQR$. *Triangles* are patients who fall outside the $Q_{1,3} \pm 1.5 \times IQR$ for differences in baseline √ RPE atrophy. *Dashed line*: 45° line of perfect agreement. Q_1, first interquartile; Q_3, third interquartile; IQR, interquartile range.

The Bland-Altman plot (Supplementary Fig. S3A) showed inter-eye differences up to 2.49 mm of baseline √ RPE atrophy area. An inter-eye difference below $Q_1 - 1.5 \times IQR$ or above $Q_3 + 1.5 \times IQR$ (Supplementary Fig. S3B), that is, discordant RPE atrophy at baseline, was identified in eight patients (intermediate-onset STGD1, four patients; late-onset STGD1, four patients). The overall inter-eye agreement (ρ_c) of baseline RPE atrophy was 0.876 (95% CI, 0.806–0.921).

Discordance of RPE Atrophy Progression Rates

Inter-Eye Correlations of RPE Atrophy Progression. The median follow-up time was 3.9 years (range, 0.5–9.7), of which the distribution did not differ between all disease-onset categories. The mean √ RPE atrophy progression rates in the right and left eyes were 0.21 (±0.20) mm/y and 0.20 (±0.21) mm/y, respectively. Thirty-five right eyes and 31 left eyes were identified as the eye with the slowest progression rate. Two pairs of eyes showed no progression in 3.0 and 3.4 years, respectively. The progression rates of √ RPE atrophy correlated between the left and right eyes with $\rho = 0.766$ and increased with earlier disease-onset groups ($P = 9.8 \times 10^{-7}$). Evaluating the inter-eye agreement in progression of RPE atrophy, the agreement between the eyes was $\rho_c = 0.765$ (95% CI, 0.645–0.847) (Fig. 1).

Discordant Progression Rates of RPE Atrophy. Twelve out of 68 patients (early-onset STGD1, two patients [14%]; intermediate-onset STGD1, four patients [12%]; late-onset STGD1, six patients [29%]) had discordant RPE atrophy progression rates between their eyes by differences below $Q_1 - 1.5 \times IQR$ or above $Q_3 + 1.5 \times IQR$. In four of these patients, the eye with the largest RPE atrophy area progressed faster than the other eye, thus increasing inter-eye discordance of RPE atrophy over time (mean difference, 0.26 [±0.10] mm/y; Fig. 2A). In the other eight patients, the eye with the smallest RPE atrophy area progressed faster than the other eye, therefore reducing inter-eye discordance of RPE atrophy (mean difference, 0.30 [±0.12] mm/y; Fig. 2B). The remaining 56

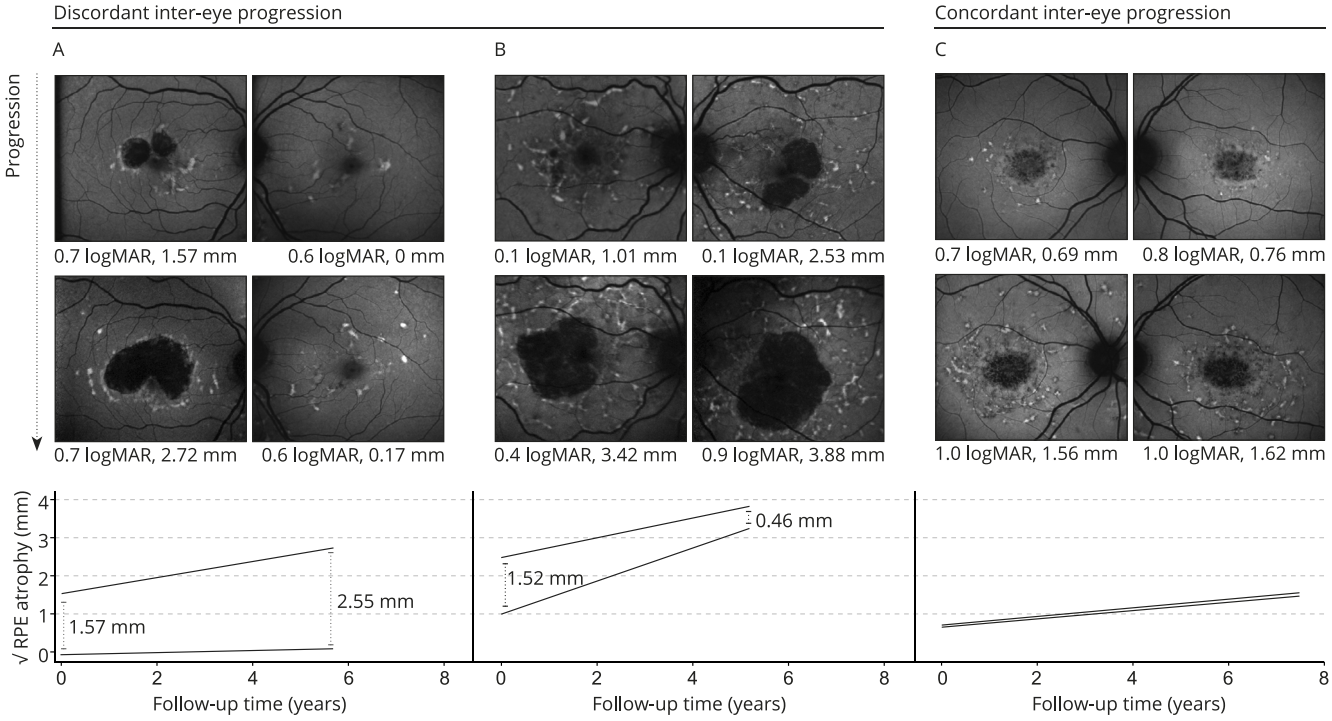

Figure 2. Concordant and discordant inter-eye progression in Stargardt disease. **(A)** 60-year old female with a disease duration of 1 year and increasing inter-eye differences. *ABCA4* variants: c.5461-10T>C:p.[Thr1821Valfs*13,Thr1821Aspfs*6]/c.2757A>C:p.(Glu919Asp). **(B)** Eighty-one-year old female with a disease duration of 26 years and decreasing inter-eye differences. *ABCA4* variants: c.5196+1G>T:p.(?)/+. **(C)** Twenty-six-year old female with a disease duration of 6 years and similar progression rates between eyes. *ABCA4* variants: c.1853G>A;4297G>A:p.(Gly618Glu;Val1433Ile)/c.2588G>C:p.[Gly863Ala;Gly863del].

Investigative Ophthalmology & Visual Science

Downloaded from iovs.arvojournals.org on 06/28/2019

Table 2. Proportions of Combinations of *ABCA4* Variants and Discordant RPE Atrophy Progression

ABCA4 Variant Combination	RPE Atrophy Progression		
	No Discordance	Discordant	Inter-Eye Correlation (Pearson's ρ)
1. Pathogenic/pathogenic	3	1	0.995
2. Pathogenic/likely pathogenic	21	4	0.790
3. Likely pathogenic/likely pathogenic	9	0	0.597
4. Pathogenic/*	12	3	0.079
5. Likely pathogenic/*	11	4	0.346

* The second *ABCA4* variant was likely benign, of unknown pathogenicity, or not found.

patients had similar progression rates between their eyes (mean difference, 0.05 [±0.04] mm/y, within $Q_{1,3} \pm 1.5 \times IQR$; Fig. 2C).

Baseline RPE Atrophy and Genetic Associations With Discordant RPE Atrophy Progression. Discordant RPE atrophy at baseline was associated with discordant RPE atrophy progression (odds ratio, 6.50; 95% CI, 1.35–31.34); this association was not found for discordant BCVA at baseline (odds ratio, 0.33; 95% CI, 0.04–2.85).

Furthermore, decreasing pathogenicity of *ABCA4* variant combinations were significantly associated with increasing discordant inter-eye progression ($P = 0.007$). Proportions and correlations are depicted in Table 2.

Power Calculations of a Theoretical Intervention Trial

The power of a paired-control intervention trial will depend on the strength of correlations between pairs, that is, the left and right eye of each patient, and the expected treatment effect. For each two-fold increase in expected treatment effect, approximately a four-fold decrease in patient numbers is needed for a study at equal power. Stronger inter-eye correlations will have a linear beneficial effect on the number needed to include. The impact on these numbers is highest when a relatively modest treatment effect is expected. For instance, a correlation of $\rho = 0.766$ would require 44 patients, whereas this number is reduced to 20 in the case of a correlation of $\rho = 0.9$ (Fig. 3). The specific inclusion criteria, for example, disease onset, *ABCA4* variant combinations, and baseline discordance can significantly affect the number needed to include.

Discussion

Based on longitudinal FAF data in our current study, the overall agreement of inter-eye RPE atrophy progression in STGD1 was only moderate; it was highest in early-onset STGD1 and lowest in late-onset STGD1. Discordant progression rates were found in 12 out of 68 (17.6%) patients, which is surprisingly high given that STGD1 is assumed to be a symmetrical inherited retinal disease. Discordant progression rates resulted in eyes either converging or diverging in atrophy size. Discrepancies of RPE atrophy progression rates were associated with discrepancies of RPE atrophy at baseline and less pathogenic *ABCA4* variant combinations.

Autosomal retinal dystrophies are expected to be symmetrical owing to the similar genetic and environmental background of both eyes. The majority of STGD1 patients exhibit bilateral symmetry in retinal features. Chen et al.[12] illustrated this symmetry in left and right eyes of 24 STGD1 patients; they had highly correlated areas of RPE atrophy (Pearson's $\rho =$

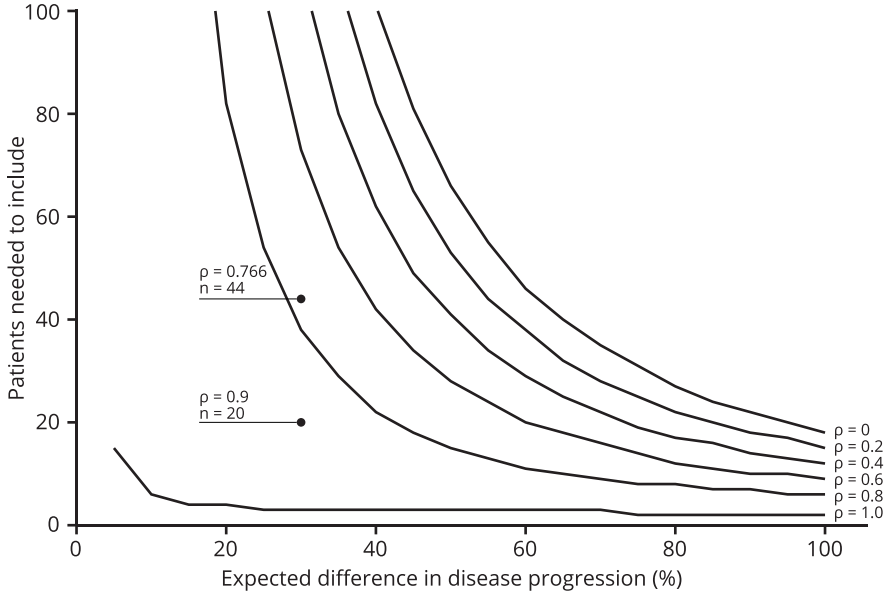

Figure 3. A sensitivity analysis for the power calculation of a theoretical intervention trial. Assuming a 30% reduction in disease progression (treatment effect), 44 patients are needed (inter-eye correlation $\rho = 0.766$; $\beta = 0.20$, $\alpha = 0.05$, two-sided paired samples *t*-test). The sample size will decrease to 20 in the case of an inter-eye correlation of 0.9. In the case of a correlation in disease progression of 1, 0.8, 0.6, 0.4, 0.2, and 0 between left and right eyes, 3, 38, 73, 108, 143, or 178 patients are needed, respectively.

Investigative Ophthalmology & Visual Science

Downloaded from iovs.arvojournals.org on 06/28/2019

0.998). McBain et al.[11] studied the atrophy progression rates in 12 STGD1 patients, reporting a strong inter-eye correlation (Spearman's $\rho = 0.846$). In our cohort, these inter-eye correlations of RPE atrophy were substantially lower, but they can be explained by inclusion of late-onset STGD1 patients, which decreased the overall correlation. Inter-eye correlations of late-onset STGD1 were previously estimated to be moderate ($\rho = 0.52$).[20] When late-onset STGD1 patients are excluded, our inter-eye correlations were similar to those reported by others.

Previous studies were limited by standard analyses of correlations, which cannot address the absolute symmetry within a patient. In contrast, we used Lin's concordance correlation coefficients and descriptive Bland-Altman plots, which are more appropriate and previously described in age-related macular degeneration.[27] In addition, there is an inherent increase in variability of inter-eye differences when the magnitude of atrophic areas increases. We corrected this by expressing the inter-eye differences as the square root, thus the differences were proportional to the magnitude of measurements. Moreover, square root transformation corrected baseline dependence, which was reported previously with an average atrophy enlargement increase of 0.016 mm^2/y for each month of follow-up.[10]

Although we found that progression rates for atrophy are more likely to be discordant in eyes that differ more at baseline, progression rates are rather unpredictable between patients and between eyes within a patient. McBain et al.[11] suggested that electroretinography could predict the rate of atrophy progression, but they did not account for baseline atrophy size. It would be interesting if discordance in electroretinography between eyes of a patient would also predict inter-eye differences in progression, independent of their baseline atrophy size.[10] Burke et al.[31] indicated that changes on optical coherence tomography would precede RPE atrophy and may thus predict the rates of atrophy progression. These potential predictors for disease progression need to be addressed in future work.

The lower inter-eye correlations in older patients could be explained by the increased time within which stochastic factors, for example, small initial differences leading to significant differences later, can influence phenotypic expression. Differences in *ABCA4* variant expression may alter disease severity between eyes with mild variants, which can have a slightly different pathogenicity. In contrast, differences in expression would not influence progression speed much in severe *ABCA4* combinations as both variants would cause an equally severe phenotype.

The statistical power of a randomized controlled trial increases when differences are measured between correlated left and right eyes. To this extent, we recommend a fellow-eye paired trial design for retinal dystrophies, for example, as applied in a phase II gene therapy trial for choroideremia with 30 patients enrolled (ClinicalTrials.gov, NCT02407678). To achieve 80% statistical power in this trial, an effect size of at least 0.53 is required.[32] For the same expected effect size, a patient-controlled trial would need 58 patients in each arm.[33] Even in multicenter trials, such high sample sizes are difficult to obtain in rare retinal dystrophies. However, it is important to bear in mind that a fellow-eye paired control is impossible for pharmaceutical strategies in which both eyes of a patient are being treated (ClinicalTrials.gov, NCT02402660). Furthermore, it is preferred that an effect on relatively slow retinal degeneration is detected to identify a potential long-term benefit rather than a temporary gain of visual function.[34]

A therapeutic trial will gain a major advantage from a fellow-eye control in early-onset STGD1 because of their high inter-eye correlations. However, discordance was also present in some of these younger patients. As the progression can be better predicted in similar rather than in discordant eyes, retinal asymmetry needs to be considered as an exclusion criterion for small early-phase trials. Such stringent criteria will increase the chance of detecting efficacy with fewer patients. Criteria would include early-onset STGD1 patients with concordant retinal abnormalities between their eyes carrying severe *ABCA4* variants; not only do these patients have the highest inter-eye symmetry in disease progression, but they are also expected to have the most severe disease course.[1,2] In these patients, therapy will potentially provide the most benefit, and in these patients, its effect has the highest chance to be detected.

Acknowledgments

The authors thank the Diagnostic Image Analysis Group, Department of Radiology and Nuclear Medicine, Radboud University Medical Center (Nijmegen, The Netherlands) for providing the image analysis algorithm.

Supported by the Stichting A.F. Deutman Researchfonds Oogheelkunde, Nijmegen, The Netherlands; Nederlandse Oogonderzoek Stichting, Nijmegen, The Netherlands; and by the following foundations that contributed through UitZicht: Stichting MD fonds, Landelijke Stichting voor Blinden en Slechtzienden, and Oogfonds. The funding organizations had no role in the design or conduct of this research. They provided unrestricted grants.

Disclosure: **S. Lambertus**, None; **N.M. Bax**, None; **J.M.M. Groenewoud**, None; **F.P.M. Cremers**, None; **G.J. van der Wilt**, None; **B.J. Klevering**, None; **T. Theelen**, None; **C.B. Hoyng**, Allergan (R), Bayer Healthcare (F, R), Novartis (R), Roche (R), Sanofi (R), Topcon (R)

References

1. Fujinami K, Zernant J, Chana RK, et al. Clinical and molecular characteristics of childhood-onset Stargardt disease. *Ophthalmology*. 2015;122:326–334.
2. Lambertus S, van Huet RA, Bax NM, et al. Early-onset Stargardt disease: phenotypic and genotypic characteristics. *Ophthalmology*. 2015;122:335–344.
3. Westeneng-van Haaften SC, Boon CJ, Cremers FP, Hoefsloot LH, den Hollander AI, Hoyng CB. Clinical and genetic characteristics of late-onset Stargardt's disease. *Ophthalmology*. 2012;119:1199–1210.
4. Yatsenko AN, Shroyer NF, Lewis RA, Lupski JR. Late-onset Stargardt disease is associated with missense mutations that map outside known functional regions of *ABCR* (*ABCA4*). *Hum Genet*. 2001;108:346–355.
5. Rotenstreich Y, Fishman GA, Anderson RJ. Visual acuity loss and clinical observations in a large series of patients with Stargardt disease. *Ophthalmology*. 2003;110:1151–1158.
6. Allikmets R, Singh N, Sun H, et al. A photoreceptor cell-specific ATP-binding transporter gene (*ABCR*) is mutated in recessive Stargardt macular dystrophy. *Nat Genet*. 1997;15:236–246.
7. Weng J, Mata NL, Azarian SM, Tzekov RT, Birch DG, Travis GH. Insights into the function of Rim protein in photoreceptors and etiology of Stargardt's disease from the phenotype in *abcr* knockout mice. *Cell*. 1999;98:13–23.
8. Stargardt K. Über familiäre, progressive degeneration in der makulagegend des auges. *Albrecht Von Graefes Arch Klin Exp Ophthalmol*. 1909;71:534–550.
9. Armstrong JD, Meyer D, Xu S, Elfervig JL. Long-term follow-up of Stargardt's disease and fundus flavimaculatus. *Ophthalmology*. 1998;105:448–457.
10. Fishman GA, Stone EM, Grover S, Derlacki DJ, Haines HL, Hockey RR. Variation of clinical expression in patients with

Investigative Ophthalmology & Visual Science

Downloaded from iovs.arvojournals.org on 06/28/2019

Stargardt dystrophy and sequence variations in the *ABCR* gene. *Arch Ophthalmol*. 1999;117:504–510.

11. McBain VA, Townend J, Lois N. Progression of retinal pigment epithelial atrophy in Stargardt disease. *Am J Ophthalmol*. 2012;154:146–154.
12. Chen B, Tosha C, Gorin MB, Nusinowitz S. Analysis of autofluorescent retinal images and measurement of atrophic lesion growth in Stargardt disease. *Exp Eye Res*. 2010;91:143–152.
13. Fujinami K, Sergouniotis PI, Davidson AE, et al. Clinical and molecular analysis of Stargardt disease with preserved foveal structure and function. *Am J Ophthalmol*. 2013;156:487–501.
14. Han Z, Conley SM, Naash MI. Gene therapy for Stargardt disease associated with *ABCA4* gene. *Adv Exp Med Biol*. 2014;801:719–724.
15. Schwartz SD, Hubschman JP, Heilwell G, et al. Embryonic stem cell trials for macular degeneration: a preliminary report. *Lancet*. 2012;379:713–720.
16. Charbel Issa P, Barnard AR, Herrmann P, Washington I, MacLaren RE. Rescue of the Stargardt phenotype in *Abca4* knockout mice through inhibition of vitamin A dimerization. *Proc Natl Acad Sci U S A*. 2015;112:8415–8420.
17. Cukras CA, Wong WT, Caruso R, Cunningham D, Zein W, Sieving PA. Centrifugal expansion of fundus autofluorescence patterns in Stargardt disease over time. *Arch Ophthalmol* 2012;130:171–179.
18. Fujinami K, Lois N, Mukherjee R, et al. A longitudinal study of Stargardt disease: quantitative assessment of fundus autofluorescence, progression, and genotype correlations. *Invest Ophthalmol Vis Sci*. 2013;54:8181–8190.
19. Lois N, Halfyard AS, Bird AC, Holder GE, Fitzke FW. Fundus autofluorescence in Stargardt macular dystrophy-fundus flavimaculatus. *Am J Ophthalmol*. 2004;138:55–63.
20. Lambertus S, Lindner M, Bax NM, et al. Progression of late-onset Stargardt disease. *Invest Ophthalmol Vis Sci*. 2016;57:5186–5191.
21. Teussink MM, Lee MD, Smith RT, et al. The effect of light deprivation in patients with Stargardt disease. *Am J Ophthalmol*. 2015;159:964–972.
22. Boon CJ, Jeroen Klevering B, Keunen JE, Hoyng CB, Theelen T. Fundus autofluorescence imaging of retinal dystrophies. *Vision Res*. 2008;48:2569–2577.
23. Feuer WJ, Yehoshua Z, Gregori G, et al. Square root transformation of geographic atrophy area measurements to eliminate dependence of growth rates on baseline lesion measurements: a reanalysis of age-related eye disease study report no. 26. *JAMA Ophthalmol* 2013;131:110–111.
24. Cohen J, Cohen, P. Fisher's z′ transformation and comparisons between independent rs. In: *Applied Multiple Regression/Correlation Analysis for the Behavioral Sciences*. Hillsdale, NJ: Erlbaum; 1983:53–55.
25. Bland JM, Altman DG. Statistical methods for assessing agreement between two methods of clinical measurement. *Lancet*. 1986;1:307–310.
26. Lin LI. A concordance correlationc to evaluate reproducibility. *Biometrics*. 1989;45:255–268.
27. Fleckenstein M, Adrion C, Schmitz-Valckenberg S, et al. Concordance of disease progression in bilateral geographic atrophy due to AMD. *Invest Ophthalmol Vis Sci*. 2010;51:637–642.
28. Lin L, Hedayat AS, Sinha B, Yang M. Statistical methods in assessing agreement: Models, issues, and tools. *J Am Stat Assoc*. 2002;97:257–270.
29. Lin LI. A note on the concordance correlation coefficient. *Biometrics*. 2000;56:324–325.
30. McBride GB. *A Proposal for Strength-of-Agreement Criteria for Lin's Concordance Correlation Coefficient*. NIWA Client Report: HAM2005-06. Hamilton New Zealand: National Institute of Water & Atmospheric Research Ltd, 2005.
31. Burke TR, Rhee DW, Smith RT, et al. Quantification of peripapillary sparing and macular involvement in Stargardt disease (STGD1). *Invest Ophthalmol Vis Sci*. 2011;52:8006–8015.
32. O'Brien RG, Muller KE. Unified power analysis for t-tests through multivariate hypotheses. In: Edwards LK, ed. *Applied Analysis of Variance in Behavioral Science*. New York: Marcel Dekker; 1993:297–344.
33. Dixon WJ, Massey FJJ. *Introduction to Statistical Analysis*. 4th ed. New York: McGraw Hill; 1983.
34. Cideciyan AV, Jacobson SG, Beltran WA, et al. Human retinal gene therapy for Leber congenital amaurosis shows advancing retinal degeneration despite enduring visual improvement. *Proc Natl Acad Sci U S A*. 2013;110:E517–E525.

Investigative Ophthalmology & Visual Science

Downloaded from iovs.arvojournals.org on 06/28/2019